Antimicrobial evaluation of composite films based on polyvinyl alcohol/triazolopyrimidenes/selenium nanoparticles

Ahmed E. Abdelhamid[a], Reham R. Khattab[b], Samira A. Swelam[b], Abdelmohsen M. Soliman[c], Sherein I. Abd El-Moez[d], Sherien F. Belasy[e], Ahmed A. El-Sayed[b]

[a]Polymers and Pigments Department, National Research Centre, Dokki, [b]Photochemistry Department, National Research Centre, [c]Therapeutic Chemistry Department, National Research Centre, Dokki, [d]Microbiology and Immunology Department, National Research Centre, Dokki, Giza, [e]Medical Microbiology and Immunology Department, National Hepatology and Tropical Medicine Research Institute (NHTMRI), Gothi, Egypt

Correspondence to Ahmed A. El-Sayed, PhD, National Research Centre, Photochemistry Department, Industrial Chemical Institute, Cairo, Egypt, P.O. Box: 12611, Mail: 33 Al-Bohouth Street, National Research Centre, Dokki, Cairo, Egypt. Tel: +00201008653440; fax: +202 3337 09 31; e-mail: ahmedcheme4@yahoo.com

Received: 26 July 2023
Revised: 9 August 2023
Accepted: 20 August 2023
Published: 2 February 2024

Egyptian Pharmaceutical Journal 2024, 23:35–45

Background
Using ultrasonic waves, a multi-component reaction of aminotriazole, carbonyl compounds and cyanoester derivatives, triazolopyrimidines are created with outstanding yields in a shorter amount of time. Selenium nanoparticles (SeNPs) with outstanding biological activity combined with triazolopyrimidine can imply promising materials for different biological applications.
Objective
Synthesis of triazolopyrimidine compounds conjugated with SeNPs and their incorporation into biodegradable polyvinyl alcohol for antimicrobial application were investigated.
Methods
The synthesized triazole derivatives were used in the synthesis of *in situ* SeNPs. The synthesized triazole derivatives and SeNPs were blended with polyvinyl alcohol (PVa) to prepare composite films. All synthesized compounds were confirmed using FT-IR, ^{1}H-NMR, mass spectroscopy and elemental analysis. The prepared PVa composite films with nanoparticles were tested against Gram-positive (+ ve) and Gram-negative (–ve) bacteria.
Results
The treated PVA with the SeNPs showed high biological efficiency compared with PVA treated with triazole derivatives.

Keywords:
antibacterial, composite film, polyvinyl alcohol, selenium nanoparticles, triazole derivatives

Egypt Pharmaceut J 23:35–45

1687-4315

Permission to publication: The final version submitted to the journal is accepted by the authors.

Introduction

The selenium element (Se) is extremely important and benefits in the interest of human health, microbes and animals. In recent decades, selenium nanoparticles (SeNPs) have been gaining attention by many researchers because of their ability to be compatible with living tissue or a living system, their low toxicity, available for the intended biological destination and their high biological activity, so the use of SeNPs is in a large range in medical and biological applications [1–4]. Heterocyclic compounds, particularly those having nitrogen atoms, are important molecules in organic chemistry due to their extraordinary activity, especially anticancer activity [5–12]. Triazole is an important heterocyclic moiety, widely used in many bioactive compounds and synthetic pharmaceuticals [13–16]. Triazole fused with other heterocycles, such as pyrimidine, is found in the core of various pharmaceuticals and natural products, and has a wide range of biological activities, including anticancer effects [14,17–22]. Some reports related to the preparation of triazolopyrimidine have appeared, however, it often requires drastic conditions, long reaction times and the synthesis pathways are complex and often require volatile organic solvents [23]. Thus, a new route to the synthesis of nanomaterial using bio-inspired and greener methods is one of the most fascinating aspects of current materials science. There is a growing need to provide high-yielding, low-cost, non-toxic, and ecologically friendly products' synthetic methods for small-dimension materials, which can be met by biological approaches. Therefore, we focused on developing an environmentally friendly synthetic method for substituted triazolopyrimidines [24]. Recently, lemon juice has been used as a biocatalyst in the synthesis of heterocyclic compounds in our research because it is

 DOI: 10.4103/epj.epj_172_23

environmentally friendly, non-toxic, readily available and inexpensive. Encapsulation or incorporation of bioactive compounds and nanoparticles into a biocompatible polymer was largely utilized to minimize the side effect of these compounds on the living cells [25,26]. Biocompatible polymers can be found naturally such as chitosan, alginate, collagen and gelatin, or synthetic ones such as polyvinyl pyrrolidone polyethylene glycol and polyvinyl alcohol [27,28]. PVA is a vinyl polymer with exclusively carbon-carbon bonds with branched hydroxyl groups. PVA (polyvinyl alcohol) is a water-soluble synthetic compound that is commonly used in paints, adhesive, textile, paper industry, food packaging industry and cosmetics [29,30]. Enzymatic degradation of polyvinyl alcohol is performed by Acinetobacter, Flavobacterium and Pseudomonas bacterial strains having alcohol peroxidase activity [31]. Therefore, in this study, we reported a one-pot ternary reaction between amino triazole, carbonyl compounds and active methylene compounds in the presence of lemon juice using a sono-synthesized method for preparation of bioactive triazolopyrimidines [24,32]. SeNPs were also synthesized using triazolopyrimidines as a stabilizing and co-reducing agent for the synthesis of bioactive SeNPs. The incorporation of these triazolopyrimidines and SeNPs into a PVa film matrix was investigated towards different Gram-positive and Gram-negative bacterial strains.

Materials and methods

TLC stands for thin layer chromatography employing aluminium UV fluorescent silica gel. Merck Kieselgel 60 F245 was reapplied to the sheets, which was used to monitor all reactions. It was viewed with an ultraviolet lamp and iodine vapour. All melting points were obtained using an electro-thermal IA 9100 instrument (Shimadzu, Japan) and are uncorrected. The Micro analytical center (Faculty of Science, Cairo University, Cairo, Egypt) performed the micro analyses. IR spectra were collected using KBr discs on a JASCO FT/IR 6100 Japan spectrometer (National Research Centre, Cairo, Egypt). ^{1}H-NMR spectra were measured in DMSO, $CDCl_3$ or $CDCl_3/CF_3COOD$ using a JEOL EX-270 at 270 MHz, a JEOL ECA-500 at 500 MHz and a JEOL ECA-125 at 125-MHz spectrometer (National Research Centre, Cairo, Egypt). The chemical shifts were measured in parts per million (ppm) against tetramethylsilane (TMS) as an internal reference, and the coupling constant J was measured in hertz (Hz). The GCMS Finnigan mat SSQ 7000 spectrometer (National Research Centre, Cairo, Egypt) was used to record the mass spectra. The elemental analyzer (EDAX AMETEK Inc., Mahwah, NJ, USA) was used with acceleration voltages of 15 kV at the National Research Centre in Cairo, Egypt. Fine chemicals of analytical grade were used. Aldrich selenium sulphate (H_2SeO_3) with ascorbic acid (99%).

Conventional method for 4a-b synthesis

In ethanol (25 ml), an equimolecular amount of 3-amino-1,2,4-triazole (1) (0.083 g, 0.001 mol), aldehyde (2) [5-methyl furfuraldehyde or 3, 4, 6-trimethoxybenzaldehyde] (0.001 mol) and (3) ethyl cyanoacetate to produce 4a or malononitrile to produce 4b was refluxed for about 5 days. However, there was no reaction after the intermediate stage. The reaction was then resumed after the addition of 4-5 drops of lemon juice; the colour quickly changed to yellow, and the progress was observed using TLC. The reaction mixture was left at room temperature overnight. The precipitate that formed was filtered, washed with ethanol, then dried and recrystallized from ethanol. 4a, yield 75%; mp 160–162°C, 4b, yield 70%; mp 168–170°C.

Ultrasonic technique for 4a-b synthesis

In the bottom of a conical flask with water and a few drops of lemon juice (10 ml), equimolarr quantities of 3-amino-1,2,4-triazole (1) (0.083 g, 0.001 mol), 5-methyl furfuraldehyde (2) (0.011 g, 0.001 mol) and (3) ethylcyanoacetate were added. The combination was immersed in ultrasonic waves for 3 h at room temperature using an ultrasonic bath (230 V, 33-KHz output frequencies). During the reaction, the product started to separate. The crystalline substance was filtered and determined to be pure on TLC, indicating that no additional recrystallization was required.

Ethyl-5-amino-7-(2,4,5-trimethoxyphenyl)-7,8-dihydro [1,2,4]triazolo[4,3-a]pyrimidine-6-carboxylate 4a

Yellow powder, IR (KBr, ν, cm-1); 3420 (NH_2), 3141 (-NH), 3091 (-CH, aromatic), 2921 (-CH, aliphatic), 1714 (C=O), ^{1}H-NMR (DMSO-d_6, δ ppm): 8.01 (s, 1H, -CH, triazole ring), 7.62 (s, 1H, -NH, D_2O exchangeable), 7,38 (s, 1H, -CH, aromatic), 6.95 (s, 2H, $-NH_2$, D_2O exchangeable), 6.89 (s, 1H, -CH aromatic), 4.95 (s, 1H, -CH), 4.25 (q, 2H, J=5.3 Hz, $-OC\underline{H}_2CH_3$), 3.98 (s, 3H, $-OCH_3$), 3.94 (s, 3H, $-OCH_3$), 3.92 (s, 3H, $-OCH_3$), 1.30 (t, 3H, J=5.3 Hz, $-OCH_2C\underline{H}_3$); MS (m/z, %), 376.34 (M^{+1}, 18.81%), 375.25 (M^+, 25.43%), Anal; Calcd; for, $C_{17}H_{21}N_5O_5$ (375.39): C, 54.39%; H, 5.64%; N, 18.66%; Found: C, 54.33%; H, 5.62%; N, 18.75%.

5-Amino-7-(furan-2-yl)-7,8-dihydro-[1,2,4]triazolo[4,3-a] pyrimidine-6-carbonitrile (4b)

Brown crystals, IR (KBr, ν, cm^{-1}); 3428 (-NH_2), 2218 (C=N), 1060 (C=C); ^{1}H-NMR (DMSO-d_6, δ ppm): 8.03 (s, 1H, -CH, triazol ring), 7.51 (s, 1H, -NH), 7.45 (d, 1H, J=2.5 Hz, CH, furan ring), 6.52 (d, 1H, J=2.5 Hz, CH, furan ring), 5.02 (s, 2H, -NH_2,D_2O exchangeable), 4.87 (s, 1H, -CH); MS (m/z, %), 243.11 (M^{+1}, 50.44%), 242,15(M^+, 89.23%); Anal. Calcd; for $C_{10}H_8N_6O$ (228.22): C, 52.63; H, 3.53; N, 36.83; Found: 52.50; H, 3.56; N, 36.92.

Synthesis of *in situ* selenium nanoparticles (SeNPs) using synthesized heterocyclic compounds 4a, 4b

Selenious acid (H_2SeO_3, 0.013 gm., 0.01 mmol.) was solubilized in distilled water (80 ml.) in a conical flask. Compounds 4a, and 4b (0.01 g) in DMSO (10 ml) were added to the selenious acid solution, after the solution was heated to 60°C. The mixture was stirred at 60°C for 1 h; then 200 µl of 40 mM ascorbic acid was added as a catalyst to obtain the ruby red SeNP suspension. The formation of SeNPs was confirmed and evaluated by using an UV spectrophotometer, dynamic light scattering and TEM.

Polyvinyl alcohol (PVa)/triazole composite film preparation

PVa composite films in the presence or absence of triazole derivatives and SeNPs were prepared using casting evaporation technique. PVa was solubilized in pure water at 90 °C for about 4 h to obtain polymer concentration of 1%. Triazole derivative (0.02 g) was dissolved in 5 ml of DMSO and added dropwise to 20 ml of PVa solution under vigorous stirring. The polymer triazole derivative blend solution was poured into a 15-ml petridish and evaporated in an oven at 50 °C for 24 h. For selenium composite film, the suspension of SeNPs and triazoles prepared in the previous step was added to PVa solution under stirring, then poured in a petridish and dried with the same condition of PVa triazole films.

UV-VIS (ultraviolet-visible)

Ultraviolet-visible (Shimadzu spectrophotometer) was employed to monitor SeNPs production in triazolopyrimidine solution within a spectral range of 400-700 nm.

Transmission electron microscope

High-resolution transmission electron microscopy (HR-TEM) (JEOL, JEM-2100 TEM) was used to get the shape and size of SeNPs. TEM samples were made by putting a drop of SeNPs suspension on 400 mesh carbon-coated copper grid; at ambient temperature, followed by solvent evaporation.

Scanning electron microscope (SEM)

SEM was utilized to examine the surface topography of the prepared PVa composite films. It was performed using SEM (QUANTA FEG 250 ESEM). To determine the elemental constituents within the examined films, energy-dispersive x-ray (EDX) was employed using elemental analyzer (EDAX AMETEK Inc., Mahwah, NJ, USA) using acceleration voltages of 15 kV.

Dynamic light scattering (DLS)

A particle-size analyzer (Nano-ZS, Malvern Instruments Ltd., UK) was used to assess the mean diameter and size distribution of suspension samples. The suspension samples were sonicated for 10-20 min just before measurements.

Agar disc diffusion test (ADDT)

The agar disc diffusion method was used to conduct antimicrobial tests. Under aseptic conditions, sterile plates of Muller-Hinton agar (Oxoid) and potato dextrose agar were prepared. The media is then allowed to cool and solidify for 15 min. Freshly prepared bacterial and mycotic suspensions were made using reference strains/isolates. The surface of the Muller-Hinton agar plates and potato dextrose agar was then covered with 100 l of suspension containing 1×10^8 CFU/ml of pathologically tested bacteria/ mycotic strains/isolates. The material was then cut under sterile conditions into 1-cm squares, and once the reference strain had distributed, the material was placed onto the surface and pressed well to allow the spread of the active ingredient under research. After that, the inoculation plates were incubated for 24 h [33]. Antimicrobial activity was represented as inhibitory diameter zones in millimetres (mm) after incubation time. The experiment was repeated three times, and the average zone of inhibition was calculated. The zone of inhibition is determined using a measuring calibre. When there is negative inhibition, the results are reported as 'zero" ZOI. The following scales of –ve and +ve scoring were used to indicate the results: 0-6 mm (–), 7-12 mm (+), 13-18 mm (++), 19-24 mm (+++), 25-30 mm (++ ++) and 31-36 mm (+++++).

Results and discussion

Chemistry

As continuation of our ongoing research endeavours, to develop molecules of the privileged class [13], we present herein one-pot synthesis of triazolopyrimidines by reaction of a mixture of amino-triazole 1, aldehyde compounds 2, and active methylene compounds 3 with

an equimolar ratio in an aqueous medium to produce triazolopyrimidines in a convenient and rapid manner, owing to our particular interest in the use of the aqueous medium for heterocyclic synthesis. The reaction was evaluated under various reaction conditions to determine the best outcomes and optimize the procedure. Initially, we used the standard way to explore the reaction in ethanol with triethylamine catalyst and discovered that the target product was produced in low yield. Surprisingly, no product was produced when the reaction was carried out in ethanol without the use of a catalyst using the standard method. Furthermore, all of our attempts to increase yield, such as higher temperatures and longer response times, were not succeeded. To improve efficiency, we elected to run the reaction in water at mild conditions, and we noticed that the reaction went smoothly, providing the needed product in good to excellent yields. To improve the process even further, the reaction was performed in an ultrasonic bath with lemon juice as a green catalyst. Fruit juice acts as a biocatalyst in a variety of chemical reactions, and this biocatalyst satisfies all green chemistry standards. Analytical and spectral data confirmed the structure of the newly synthesized compounds (Scheme 1), as follows:

Ethyl-5-amino-7-(2,4,5-trimethoxyphenyl)-7,8-dihydro [1,2,4]triazolo[4,3-a]pyrimidine-6-carboxylate 4a

Yellow powder, IR (KBr, ν, cm-1); 3420 (NH_2), 3141 (-NH), 3091 (-CH, aromatic), 2921 (-CH, aliphatic), 1714 (C=O), ^{1}H-NMR (DMSO-d_6, δ ppm): 8.01 (s, 1H, -CH, triazole ring), 7.62 (s, 1H, -NH, D_2O exchangeable), 7,38 (s, 1H, -CH, aromatic), 6.95 (s, 2H, -NH_2, D_2O exchangeable), 6.89 (s, 1H, -CH aromatic), 4.95 (s, 1H, -CH), 4.25 (q, 2H, J=5.3 Hz, -O$\underline{CH_2}CH_3$), 3.98 (s, 3H, -OCH_3), 3.94 (s, 3H, -OCH_3), 3.92 (s, 3H, -OCH_3), 1.30 (t, 3H, J=5.3 Hz, -$OCH_2C\underline{H_3}$); MS (m/z, %), 376.34 (M^{+1}, 18.81%), 375.25(M^+, 25.43%), ;Anal; Calcd; for, $C_{17}H_{21}N_5O_5$ (375.39): C, 54.39%; H, 5.64%; N, 18.66%; Found: C, 54.33%; H, 5.62%; N, 18.75%.

5-Amino-7-(furan-2-yl)-7,8-dihydro-[1,2,4]triazolo[4,3-a] pyrimidine-6-carbonitrile (4b)

Brown crystals, IR (KBr, ν, cm^{-1}); 3428 (-NH_2), 2218 (C=N), 1060 (C=C); ^{1}H-NMR (DMSO-d_6, δ ppm): 8.03 (s, 1H, -CH, triazol ring), 7.51 (s, 1H, -NH), 7.45 (d, 1H, J=2.5 Hz, CH, furan ring), 6.52 (d, 1H, J=2.5 Hz, CH, furan ring), 5.02 (s, 2H, -NH_2,D_2O exchangeable), 4.87 (s, 1H, -CH); MS (m/z, %), 243.11 (M^{+1}, 50.44%),242,15(M^+, 89.23%); Anal. Calcd; for $C_{10}H_8N_6O$ (228.22): C, 52.63; H, 3.53; N, 36.83; Found: 52.50; H, 3.56; N, 36.92.

Scheme 1

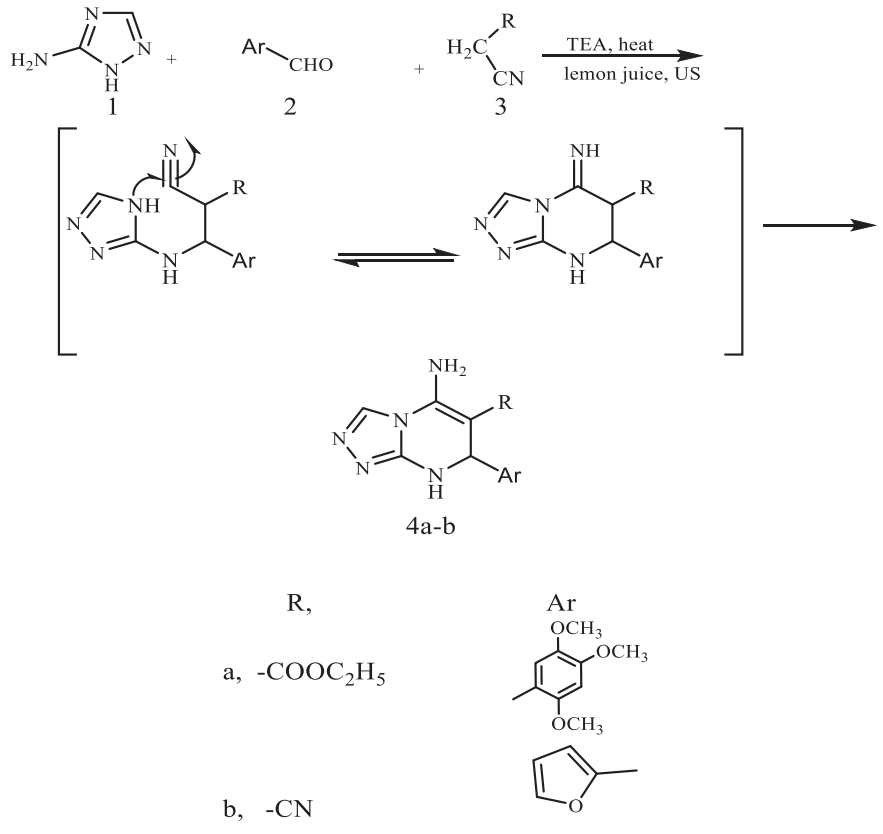

Synthesis of the triazolopyrimidine derivatives 4a,b.

Synthesis of heterocyclic selenium nanoparticles 4a-SeNPs, 4b-SeNPs using triazole derivatives (4a, 4b)

Nanoparticles have been characterized by their higher surface area to volume ratio rather than micro- or sub–micrometer-sized particles and can bind large numbers of targeting biomolecules (such as enzymes, proteins and DNA) or chemical substances (chemotherapeutic agents). As a result, the researchers attempted to synthesize unique SeNPs using the synthesized triazolopyrimidines (4a, 4b), which have adequate low decreasing but high stabilizing power during SeNP production. Organic heterocycle derivatives convert the Se^{+} cation to Se utilizing ascorbic acid as a catalyst, which serves as an aldehyde to produce SeNPs and stabilize their nanostructure from aggregation [34,35]. Organic molecules having reductive groups, such as –OH, –NH, $–NH_2$ and others, could decrease selenium cation. The synthesized structure 4a-SeNPs, 4b-SeNPs is presented in Fig. 1. SeNP compounds (4a-SeNPs, 4b-SeNPs), UV spectrophotometer, TEM method and particle-size distribution all corroborated this.

UV-visible (UV-Vis) spectrum

The solution converting to red colour after adding H_2SeO_3 to triazole derivatives was the first sign of nanoparticle production. Compounds (4a, 4b) were solubilized in DMSO and stirred for 1 h at 60°C, as demonstrated in Fig. 2a. UV-Vis spectroscopy was used to monitor the synthesis of SeNPs forming 4a-SeNPs and 4b-SeNPs suspensions. The UV-Vis absorption spectrum of SeNPs suspension is shown in Fig. 2b. The absorption spectra of the suspension solution of SeNPs showed an absorption peak at 460 nm, which corresponds to the surface plasmon resonance peaks.

Transmission electron microscope (TEM)

Transmission electron microscopy was used to establish the feature of selenium nanoparticles suspended in an aqueous solution [36]. The produced selenium nanoparticles were examined by TEM, either alone or placed onto the synthesized triazolopyrimidines (4a,b). Figure 3 depicts the existence of produced SeNPs in the tested sample. SeNPs are spherical with minimal aggregates, with particle diameters ranging from 24.98 to 60.78 nm. Figure 3a-b show that when SeNPs are put onto the examined compounds 4a,b, they distribute evenly throughout both samples. The triazolopyrimidines synthesized aided in the hindrance of agglomeration of SeNPs. The stabilizing impact of nitrogen-based molecules appears to have contributed to the creation of segregated SeNPs [37].

DLS (dynamic light scattering)

Synthesized particle size 4a-SeNPs and 4b-SeNPs was determined using dynamic light scattering (DLS) techniques. The particle-size range shown in Table 1, Fig. 4 is 50.43 and 80.90 nm on average size. DLS measurement produces larger particle sizes than TEM measurement because TEM delivers an image for a definite selected area, but DLS delivers an overall view of nanoparticles and their accumulations. Furthermore, DLS refers to the hydrated particles (hydrodynamic radius of nanoparticles) or coated particles in an aqueous solution, whereas TEM refers to nanoparticle dry diameter [38]. Mean

Figure 1

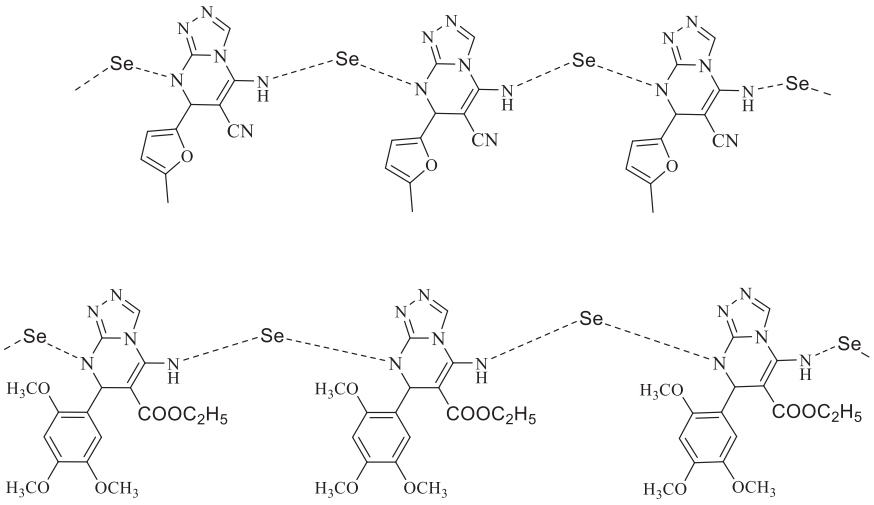

Chemical structures of synthesized Het-SeNPs 4a-SeNPs, 4b-SeNPs.

Figure 2

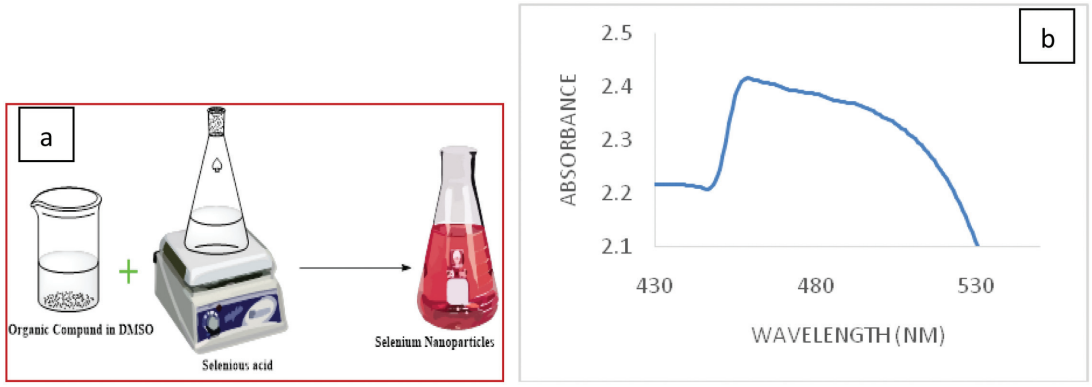

A photograph of the formed selenium nanoparticles (a) and UV-Vis spectrum of synthesized SeNPs (b).

Figure 3

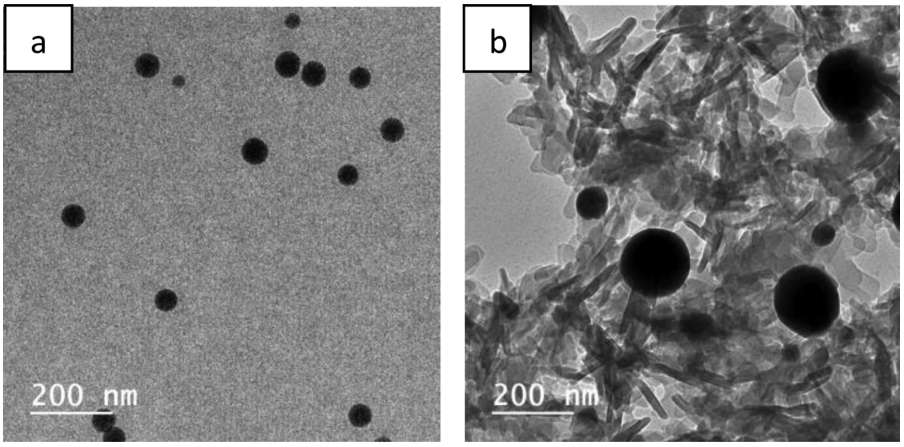

TEM of SeNPs, loaded onto (a) compound 4a, and (b) compound 4b, respectively.

particle size (MPS) of selenium nanoparticles 4a-SeNPs and 4b-SeNPs is shown in Table 1.

Table 1 Particle size of selenium nanoparticles

Compounds no.	MPS (nm)	PDI	SD
4a-SeNPs	50.43	0.666	±5.876
4b-SeNPs	60.90	0.336	±8.414

ATR-FTIR

Characterization of untreated and treated reactive functional groups composite films: PVa, PVa/4a, PVa/4a-SeNPs, PVa/4b and PVa/4b-SeNPs as illustrated in Fig. 5, samples were analyzed using FT-IR. The FTIR spectrum of untreated PVa shows distinctive peaking at 3257 cm^{-1} linked to -OH stretching, 2910 cm^{-1} related to -C-H stretching vibration and 1326 cm^{-1} corresponding to H-O-C symmetric bending vibration. The stretching vibration carbonyl (C=O) of the acetyl group of the unhydrolyzed section of the PVa structure was responsible for the peak at 1712 cm^{-1}. The infrared spectra of treated PVa/4a indicated a small shift in the peak of carbonyl bond: it appeared at 1720 cm^{-1} related to a combination of the carbonyl of the polymer and -C=O in the functional acetate (-$COOC_2H_5$) group of triazole. The -C-N bonds have a peak at 1414cm^{-1}, and the aromatic protons have a peak around 2938cm^{-1}. The IR spectra of treated PVa/4a-SeNPs revealed a peak at 1731 cm^{-1} for the -C=O in the functional acetate (-$COOC_2H_5$) group and 601 cm^{-1} for the selenium. The IR spectra of treated PVa/4b revealed a peak at 2220 cm^{-1} associated with -CN in the functional cyano group. The -C-N bonds have a peak at 1415 cm^{-1}, whereas the aromatic protons have a peak around 2939 cm-1. IR spectra for treated PVa/4b-SeNPs: the features peak at 2227 cm^{-1} for the -CN functional cyano group and 608 cm^{-1} for selenium. When untreated and treated PVa were compared, they revealed similar peaks with minor shifts in some peaks

Figure 4

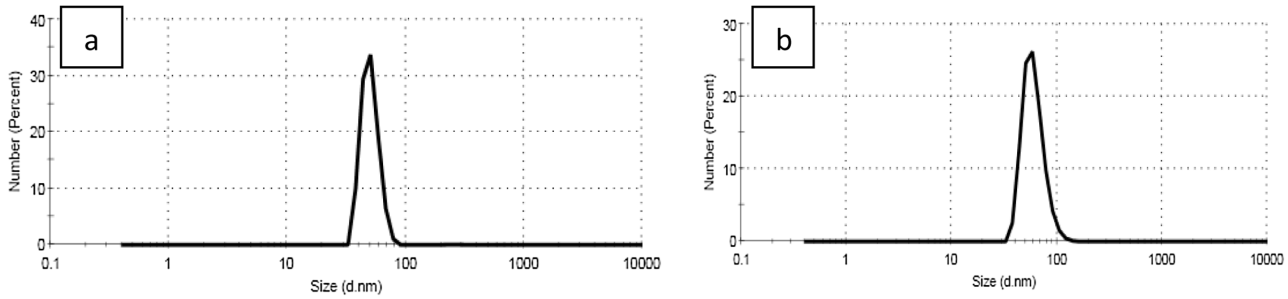

Particle size from DLS of SeNPs. a), b) SeNPs loaded onto 4a, b, respectively.

due to the low percent of treatment chemicals employed for treated PVa.

Scanning electron microscopy (SEM)

SEM images of untreated and treated 100% PVa, 4a/PVa,= and 4a-SeNP/PVa samples are shown in Fig. 6. The blank-untreated PVa morphology (Fig. 6a) showed a homogeneous and smooth surface, which resulted from casting and evaporation technique that produces dense and nonporous or rough surface [39]. Whereas the treated samples with triazole derivatives (Fig. 6b) displayed a fairly rough surface structure,

Figure 5

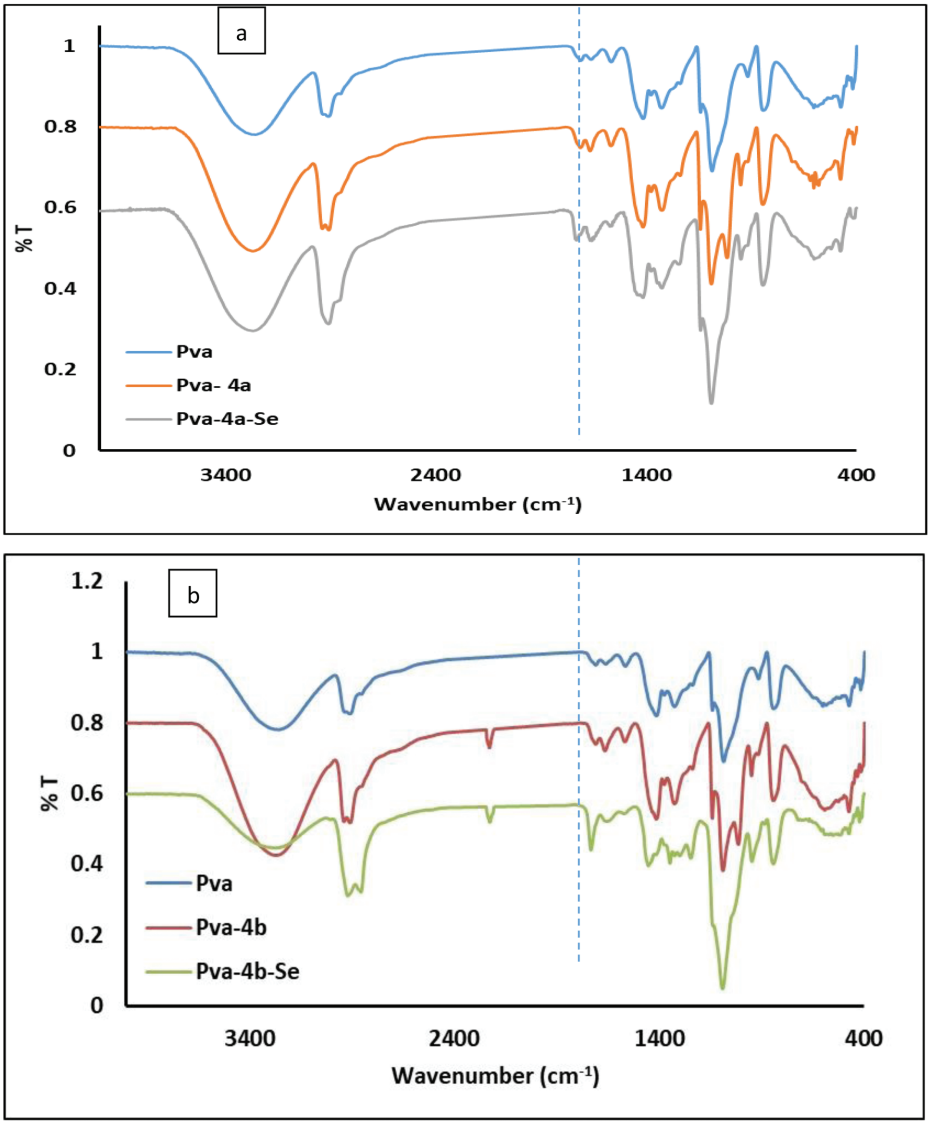

FTIR of blank and treated PVa.

Figure 6

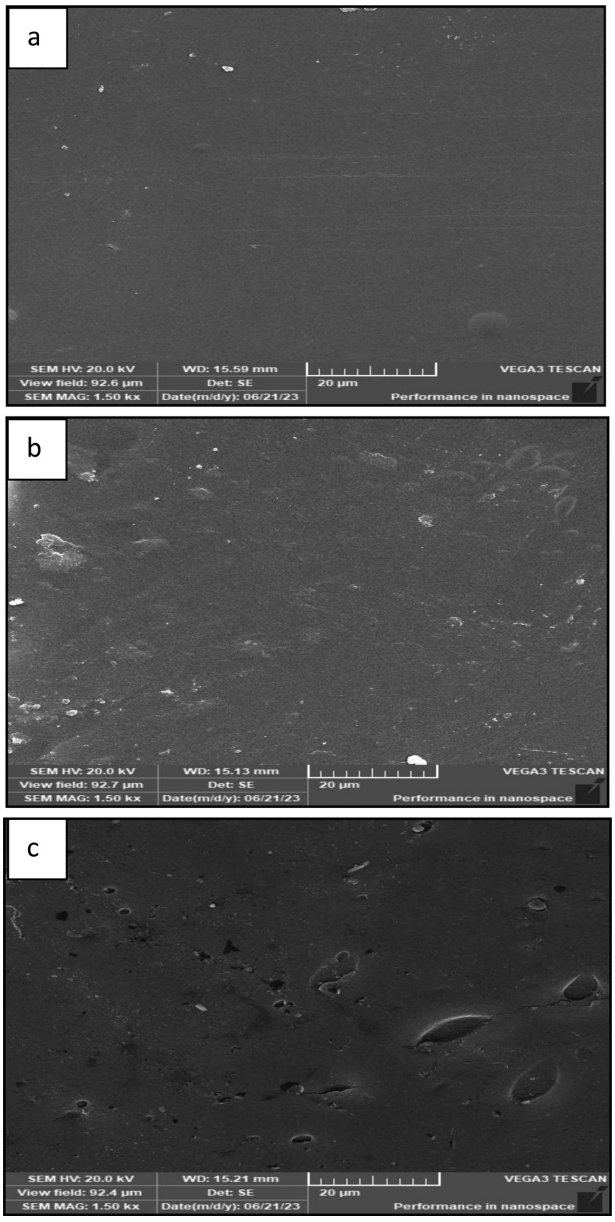

SEM of surface of (a) PVa, (b) PVa-4a and (c) PVa-4a-SeNPs films, respectively.

maybe due to changes in the microstructural properties introduced by triazole derivatives during the preparation process. The surface topography of composite films containing triazoles and SeNPs (Fig. 6c) appeared with some pores and small perceptible breaks that may be due to some aggregation of nanoparticles during the evaporation process [40].

The elemental analysis of the blank PVa in addition to PVa/4a and 4a-SeNP/PVa was explored using EDX measurement as indicated in Fig. 7. The PVa chart displayed the carbon and oxygen elements representing the chemical constitutions of polyvinyl alcohol structure. After treatment of PVa with 4a, well-representative peaks for carbon, oxygen and nitrogen were obviously displayed with percent ratio of 63.90, 35.06 and 1.04 wt%, respectively. The presence of nitrogen element in this analysis indicates the inclusion of triazole derivatives into the PVa matrix. After treatment of PVa with 4a-SeNPs, the EDX chart indicated well-characterized peaks for carbon, oxygen, nitrogen and selenium, which obviously appeared with percent ratio of 64.11, 34.34, 1.01, and 0.54 wt %, respectively. The existence of selenium and nitrogen ions in EDX measurement indicates the successful treated procedure of the PVa modification.

Antimicrobial activity

The *in vitro* antibacterial activity of the PVa blends with 4a, 4a-SeNPs, 4b and 4b-SeNPs, against three strains of Gram-positive bacteria (*S. aureus* ATCC 25923, *L. monocytogenes ATCC 7644 and methicillin resistance S. aureus (MRSA) isolate*), whereas strains of Gram-negative bacteria (*E. coli O157 ATCC 700728, Salmonella enterica Typhimurium ATCC 14028 and Shiga toxin- producing E. coli (STEC) isolate*) were investigated using disc-diffusion methods as well as mycotic reference strain/isolate, including yeast; *C.*

Table 2 Inhibition zone of tested composite films using agar disc diffusion test (ADDT)

Material tested/ Tested strains	PVa/4b	PVa/4b/Se	PVa/4a	PVa/4a/ Se	Blank PVa
Gram positive bacteria					
S. aureus ATCC 25923 (1)	0 (–)	35 (+++++)	30 (++++)	45 (+++++)	0 (–)
L. monocytogenes ATCC 7644 (4)	0 (–)	0 (–)	0 (–)	0 (–)	0 (–)
Methicillin Resistance S. aureus (MRSA) isolate (6)	0 (–)	0 (–)	0 (–)	0 (–)	0 (–)
Gram negative bacteria					
E.coli O157 ATCC 700728 **(2)**	0 (–)	30 (++++)	30 (++++)	45 (+++++)	0 (–)
Shiga Toxin producing E. coli (STEC) isolate **(8)**	0 (–)	0 (–)	0 (–)	0 (–)	0 (–)
Salmonella enterica Typhimurium ATCC 14028 **(5)**	0 (–)	0 (–)	0 (–)	0 (–)	0 (–)
Fungus					
Yeast: C. albicans ATCC 10231 **(3)**	20 s (++++)	34 (+++++)	32 (+++++)	35 (+++++)	0 (–)

0-6 mm (–), 7-12 mm (+), 13-18 mm (++), 19-24 mm (+++), 25-30 mm (++++), 31-36 mm (+++++). *S=bacteriostatic antimicrobial activity.

albicans ATCC 10231. The obtained results of antibacterial and antifungal activities are shown in Table 2. The given results of Table 2 clearly revealed that the investigated PVa/4a-SeNPs, and PVa/4b-SeNPs blends in this study have relatively promising antibacterial efficiencies. This activity was found to be significant against *S. aureus* as a the Gram-positive strains and *E.coli* as Gram-negative ones. Moreover, the potency of all tested PVa blends were extended to *C. albicans* as Yeast and showed high potent activity. Concerning the Gram-positive strains (*L. monocytogenes ATCC 7644 and methicillin resistance S. aureus (MRSA) isolate*) and Gram negative strains (*Salmonella enterica Typhimurium ATCC 14028, Shiga Toxin producing E. coli (STEC) isolate*), the antibacterial activity of PVa/4a, 4b blends under

Figure 7

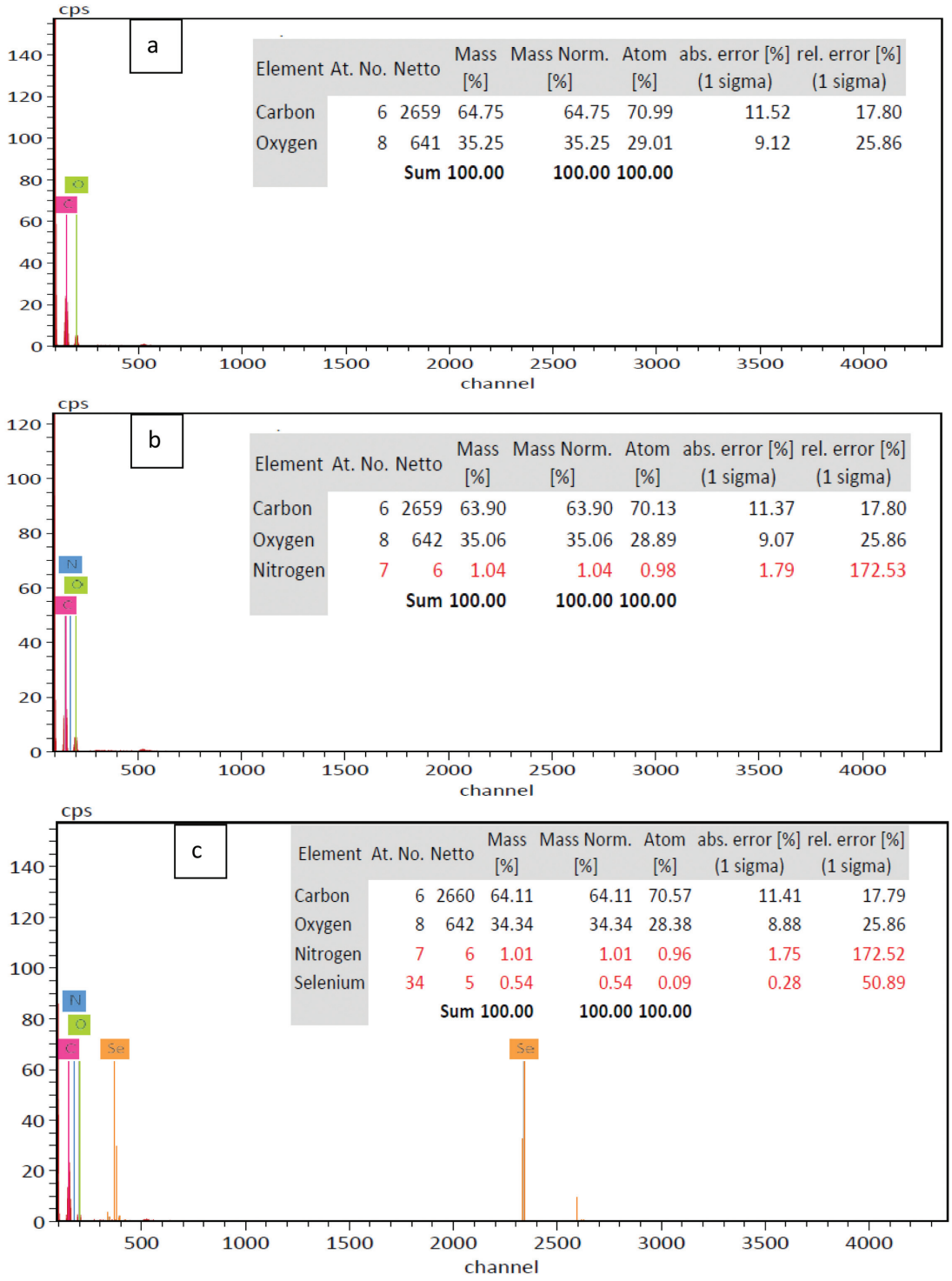

EDX analysis of (a) PVa, (b) PVa-4a and (c) PVa-4a-Se films, respectively.

investigation clearly showed no activity. The most expected important mechanism for antimicrobial actions of PVa/4a-NPs and PVa/4b-NPs may be due to the electrostatic contact between the ionic SeNPs and microbial cell surface. The observed antimicrobial activity of the investigated PVa/4a-NPs and PVa/4b-NPs blends also can be due to the presence of triazole units in the organic compound since the grafted PVa containing the triazole ring is biocompatible, biodegradable and antimicrobial [41–43].

Conclusion

Our work is focused on modification of polyvinyl alcohol (PVa) film using ecofriendly-synthesized heterocyclic triazole derivatives 4a, b and selenium nanoparticle-loaded heterocyclic triazoles (SeNPs@triazoles) for antibacterial application. PVa modification with triazole derivatives 4a, b and a one-pot synthesis of SeNPs@triazoles was used. In this study, triazole derivatives 4a, b and SeNPs@triazoles were mixed with PVa polymer solution, then casted and evaporated to obtain composite PVa films. Various characterization instruments validated the effective synthesis of triazole derivatives and the creation of nanoparticles. The blank PVa and composite PVa films were tested for their bio-activity towards G +ve bacteria and G –ve bacteria. The results showed high activity for selenium-containing films: PVa/4b-SeNPs and PVa/4a-SeNPs than containing the synthesized triazoles 4a, b only and blank PVa film.

Acknowledgements

Funding: This study received no financing from government, commercial or non-profit organizations.

Financial support and sponsorship

Nil.

Conflicts of interest

The authors declare that they have no financial or other conflicts of interest.

References

1 Bisht N, Phalswal P, Khanna PK. Selenium nanoparticles: a review on synthesis and biomedical applications. Mater Adv 2022; 3:1415–1431.

2 Cepoi L, Zinicovscaia I, Chiriac T, Rudi L, Yushin N, Grozdov D, *et al.* Modification of Some Structural and Functional Parameters of Living Culture of Arthrospira platensis as the Result of Selenium Nanoparticle Biosynthesis. Materials (Basel) 2023; 16:852.

3 Fouad H, Yang G, El-Sayed AA, Mao G, Khalafallah D, Saad M, *et al.* Green synthesis of AgNP-ligand complexes and their toxicological effects on Nilaparvata lugens. J Nanobiotechnology 2021; 19:1–17.

4 Xiao Y, Zhenzeng G, Dong E, Yan J, Liu W, Zhang G. Construction and characterization of hyperbranched polymer stabilized Se nanoparticles and its application on the antibacterial finishing of viscose nonwoven fabric. J Appl Polym Sci 2023; 140:e53500.

5 Abdelhamid AE, El-sayed AA, Swelam SA, Soliman AM, Khalil AM. Encapsulated polycaprolactone with triazole derivatives and selenium nanoparticles as promising antiproliferative and anticancer agents. ADMET DMPK 2023, accepted

6 Huang LH, Zheng YF, Song CJ, Wang YG, Xie ZY, Lai YW, *et al.* Synthesis of novel D-ring fused 7′-aryl-androstano[17,16-d][1,2,4] triazolo[1,5-a] pyrimidines. Steroids 2012; 77:367–374.

7 Bera H, Lee MH, Sun L. Synthesis, anti-thymidine phosphorylase activity and molecular docking of 5-thioxo-[1,2,4]triazolo[1,5-a][1,3,5]triazin-7-ones. Bioorg Chem 2013; 50:34–40.

8 Sun L, Bera H, Chui WK. Synthesis of pyrazolo[1,5-a][1,3,5]triazine derivatives as inhibitors of thymidine phosphorylase. Eur J Med Chem 2013; 65:1–11.

9 Hassan G, El-Sherbeny M, El-Ashmawy M, Maarouf AR. Synthesis and antitumor testing of certain new fused triazolopyrimidine and triazoloquinazoline derivatives. Arab J Chem 2017; 10:S1345–S1355.

10 Fares M, Abou-Seri SM, Abdel-Aziz HA, Safinaz ES, Abbas B, Mohieldin Magdy Youssef EF, Eladwy RA. Synthesis and antitumor activity of pyrido [2,3-d]pyrimidine and pyrido[2,3-d] [1,2,4]triazolo[4,3-a]pyrimidine derivatives that induce apoptosis through G1 cell-cycle arrest. Eur J Med Chem 2014; 83:155–166.

11 El-Gazzar YI, Georgey HH, El-Messery SM, *et al.* Synthesis, biological evaluation and molecular modeling study of new (1,2,4-triazole or 1,3,4-thiadiazole)-methylthio-derivatives of quinazolin-4(3H)-one as DHFR inhibitors. Bioorg Chem 2017; 72:282–292.

12 Abbas I, Gomha S, Elneairy M, ELaasser M, Mabrouk B. Synthesis and biological evaluation of novel fused triazolo[4,3-**a**] pyrimidinones. Turkish J Chem 2014; 39:3.

13 Elhefny EA, Elhag FA, Swelam SA. Synthesis, characterization, antitumor evaluation and molecular docking of some triazolotriazine derivatives. J Pharma Res 2014; 103:79–87.

14 Hassan AY, Sarg MT, Bayoumi AH, El-Deeb MA. Synthesis and Anticancer Evaluation of Some Novel 5-Amino[1,2,4]Triazole Derivatives. J Heterocycl Chem 2018; 55:1450–1478.

15 El-Saidi MMT, El-Sayed AA, Pedersen EB, Tantawy MA, Mohame NR, Gad W. A Synthesis, Characterization and Docking Study of Novel Pyrimidine Derivatives as Anticancer Agents. Indones J Chem 2020; 20:1163.

16 Dofe VS, Sarkate AP, Shaikh ZM, Gill CH. Ultrasound-assisted synthesis and antimicrobial activity of tetrazole-based pyrazole and pyrimidine derivatives. Heterocycl Commun 2018; 24:59–65.

17 Khattab RR, Alshamari AK, Hassan AA, Elganzory HH, El-Sayed WA, Awad HM, *et al.* Click chemistry based synthesis, cytotoxic activity and molecular docking of novel triazole-thienopyrimidine hybrid glycosides targeting EGFR. J Enzyme Inhib Med Chem 2021; 36:504–516.

18 Sáez-Calvo G, Sharma A, Balaguer de A, Barasoain I, Rodríguez-Salarichs J, Olieric N, *et al.* Triazolopyrimidines Are Microtubule-Stabilizing Agents that Bind the Vinca Inhibitor Site of Tubulin. Cell Chem Biol 2017; 24:737–750.e6

19 Mohamed MA, Khattab RR, Wasfy AAF, Riya MA, El-Kalyoubi S, Hassan NA. Synthesis and Anticancer Activity Evaluation of Some Thienopyrimidine Derivatives. Russ J Bioorganic Chem 2021; 47:1312–1323.

20 Khattab RR, Hassan AA, Kutkat OM, Abuzied KM, Hassan N. A Synthesis and Antiviral Activity of Novel Thieno[2,3-d]pyrimidine Hydrazones and Their C-Nucleosides. Russ J Gen Chem 2019; 89:1707–1717.

21 Ben Hassen M, Msalbi D, Jismy B, Elghali F, Aifa S, Allouchi H, *et al.* Three Component One-Pot Synthesis and Antiproliferative Activity of New [1,2,4] Triazolo[4,3-a]pyrimidines. Molecules 2023; 28:3917.

22 Devi MS, Srinivasan S, Muthuvel A. Selenium nanomaterial is a promising nanotechnology for biomedical and environmental remediation: A detailed review. Biocatal Agric Biotechnol 2023; 51:102766.

23 Pryadina MV, Burgart Ya. V, Saloutin VI, Kodess MI, Vlomskii EN, Rusinov VL. Synthesis of 7-alkyl(aryl)-6-alkoxycarbonyl-5-fluoroalkyl-1,2,4-tri(tetr) azolo[1,5-a]pyrimidines. Russ J Org Chem 2004; 40:902–907.

24 Khattab RR, Swelam SA, Khalil AM, Abdelhamid EA, Soliman MA, El-Sayed A. A Novel Sono-synthesized Triazole Derivatives Conjugated with Selenium Nanoparticles for cancer treatment. Egypt J Chem 2021; 64:4675–4688.

25 Abdelhamid AE, Ahmed EH, Awad HM, Ayoub MMH. Synthesis and cytotoxic activities of selenium nanoparticles incorporated nano-chitosan. Polym Bull 2023; 1–17.

26 Ahmed EH, Abdelhamid AE, Vylegzhanina ME, Volkov A. Ya, Sukhanova TE, Magdy MH. Ayoub Morphological and spectroscopical characterization of hyperbranched polyamidoamine-zwitterionic chitosan-encapsulated 5-FU anticancer drug. Polym Bull 2022; 79:137–155.

27 Abdelhamid AE, Abobakr E, Yousif A, El-Saidi MTM, El-Sayed AA. Polyvinyl Alcohol Food Packaging System Comprising Green Synthesized Silver Nanoparticles. Indones J Chem 2020; 21:350–360.

28 Ramadan ME, El-Saber MM, Adelhamid AE, El-Sayed AA. Effect of nano-chitosan encapsulated spermine on growth, productivity and bioactive compounds of chili pepper (Capsicum annuum L.) under salinity stress. Egypt J Chem 2022; 65:197–207.

29 Kandil H, Abdelhamid AE, Moghazy RM, Amin A. Functionalized PVA film with good adsorption capacity for anionic dye. Polym Eng Sci 2022; 62:145–159.

30 Finch CA. SOME PROPERTIES OF POLYVINYL ALCOHOL AND THEIR POSSIBLE APPLICATIONS. Chem Technol Water-Soluble Polym 1983; 287–306.

31 Chandra R, Rustgi R. Biodegradable polymers. Prog Polym Sci 1998; 23:1273–1335.

32 Abdelhamid AE, El-Sayed AA, Swelam SA, Soliman MA, Khalil MA. Encapsulation of Triazole Derivatives Conjugated with Selenium Nanoparticles onto Nano-Chitosan for Antiproliferative Activity towards Cancer Cells. Egypt J Chem 2022; 65:1231–1239.

33 Pinho E, Magalhães L, Henriques M, Oliveira R. Antimicrobial activity assessment of textiles: Standard methods comparison. Ann Microbiol 2011; 61:493–498.

34 Kapur M, Soni K, Kohli K. Green Synthesis of Selenium Nanoparticles from Broccoli, Characterization, Application and Toxicity. Adv Tech Biol Med 2017; 5:1–7.

35 Wadhwani SA, Gorain M, Banerjee P, Shedbalkar UU, Singh R, Kundu GC, Chopade BA. Green synthesis of selenium nanoparticles using Acinetobacter sp. SW30: Optimization, characterization and its anticancer activity in breast cancer cells. Int J Nanomedicine 2017; 12:6841–6855.

36 Ranjitha VR, Ravishankar VR. Extracellular Synthesis of Selenium Nanoparticles from an Actinomycetes Streptomyces griseoruber and Evaluation of its Cytotoxicity on HT-29 Cell Line. Pharm Nanotechnol 2018; 6:61–68.

37 Khalil AM, Georgiadou V, Guerrouache M, Mahouche-Chergui S, Samara DC, Chehimi MM, Carbonnier B. Gold-decorated polymeric monoliths: In-situ vs ex-situ immobilization strategies and flow through catalytic applications towards nitrophenols reduction. Polymer (Guildf) 2015; 77:218–226.

38 Fan W, Yan W, Xu Z, Ni H. Formation mechanism of monodisperse, low molecular weight chitosan nanoparticles by ionic gelation technique. Colloids Surf B Biointerfaces 2012; 90:21–27.

39 Chan LW, Hao JS, Wan P, Heng S. Evaluation of Permeability and Mechanical Properties of Composite Polyvinyl Alcohol Films. Chem Pharm Bull 1999; 47:1412–1416

40 Suganthi S, Vignesh S, Kalyana Sundar J, Raj V. Fabrication of PVA polymer films with improved antibacterial activity by fine-tuning via organic acids for food packaging applications. Appl Water Sci 2020; 10:1–11.

41 Abu Elella MH, Mohamed RR, Sabaa MW. Synthesis of novel grafted hyaluronic acid with antitumor activity. Carbohydr Polym 2018; 189:107–114.

42 Elella MHA, Mohamed RR, ElHafeez EA, Sabaa MW. Synthesis of novel biodegradable antibacterial grafted xanthan gum. Carbohydr Polym 2017; 173:305–311.

43 El-Hamshary H, Fouda MMG, Moydeen M, El-Newehy HM, Al-Deyab SS, Abdel-Megeed A. Synthesis and antibacterial of carboxymethyl starch-grafted poly(vinyl imidazole) against some plant pathogens. Int J Biol Macromol 2015; 72:1466–1472.